J Mater Sci (2007) 42:7819–7826
DOI 10.1007/s10853-007-1619-5

Internal friction of Niobium–Titanium–Oxygen alloys

L. M. Yu · F. X. Yin

Received: 8 July 2006 / Accepted: 15 February 2007 / Published online: 1 June 2007

Abstract The compositional and temperature dependence of the anelastic relaxation behavior in Nb–Ti–O alloys have been investigated. Using a fitting method, the complicated relaxation spectra were resolved into several elementary Debye peaks, which corresponded to the reorientation transitions of O atoms at different octahedral interstitial sites. The number of the peaks depended upon the Ti concentration. The calculation results of the site energies show that the interstitial oxygen atoms preferentially occupy the octahedral interstitial site, which has nearest-neighbor Ti substitutional atoms. Therefore, substitutional Ti solutes will markedly influence the Snoek relaxation behavior in Nb-Ti-O ternary system, even if the concentration of Ti is rather low.

Introduction

Interstitial solute atoms present in body-centered cubic (BCC) metals exhibit the well-known Snoek relaxation peak [1]. Recently, a Snoek-type high damping alloys was developed [2]. In this alloys, a high solid solution of oxygen (exceed 1.0 at%) was designed on the basis of a Nb–Ti BCC alloy. Experimental results show evidence that the Snoek damping mechanism can be applied to Nb–Ti–O alloys, and high damping capacity and high strength, induced by a certain amount of oxygen solutes, can be obtained simultaneously. It was also found that, in comparison with the theoretical single-time Debye curve, a strongly broadened damping peak was observed in the alloys. Such effect indicated that the peak has complex spectrum of relaxation times. The purpose of this work was to investigate the nature of these complex peaks and to study in more detail the influence of Ti concentration on the internal friction of Nb-based alloys.

A large number of investigations [3–7] have been made in the past 50 years for various ternary BCC alloys in order to clarify the nature of the complex damping effects. However, the explanation of these effects was quite contradictory. One explanation [8] is the occurrence of additional relaxation processes at higher temperature due to stress-induced reorientation of pairs, triplets or quadruplets of interstitials. Another explanation [9] is the asymmetrical broadening of the peak and its small shift to higher temperature due to the continuous distribution of relaxation times. Undoubtedly, a complex Snoek effect in a ternary system contains several elementary relaxation processes. Therefore, the problem-solving method of such investigation should be, first, separating a total relaxation curve into its component relaxations, and second, interpreting the relaxations using reasonable physical assumptions.

There were several works dealing with the investigation of internal friction in the Nb–Ti–O system. Szkopiak et al. showed [10, 11] that in diluted Nb–1.0 at% Ti alloys the Ti atoms acted as traps for O atoms. The latter are located in octahedral interstitial sites near Ti atoms and the activation energy for their reorientation jump increases, so that the corresponding peak shifts towards a higher temperature. The situation becomes more complicated in concentrated alloys since they feature a high probability of different configuration prior to and after the interstitial atom jump. Thus, the relaxation peaks of Nb-based alloys with high Ti contents were resolved into several elementary Debye

L. M. Yu (✉) · F. X. Yin
Innovative Materials Engineering Laboratory, National Institute for Materials Science, Tsukuba 305-0047, Japan
e-mail: liming-y-h@263.net

peaks, which were supposed to be due to Nb–O, Nb–O–O, Ti–O, Ti–O–O etc. interactions [12–14]. However, in these works, the relaxation parameters, such as the peak temperature and the activation energy, exhibited qualitative consistency but quantitative disagreement. One important reason for the mentioned discrepancy may have been the lack of a clear and rational physical model.

In the present paper, the temperature-dependence of the internal friction of a series of Nb-based alloys with different Ti content was investigated, the complex O Snoek peaks were analyzed by computer, and individual Debye constituent peaks were extracted. Then, the significance of the parameters and the nature of these peaks were discussed by using a short-range statistical model. Finally, the influence of the interaction between the substitutional (s) Ti and interstitial (i) O solutes on the relaxation behavior of Nb–Ti–O alloys were discussed.

Experimental

The design of Snoek-type high damping Nb-Ti alloys has been discussed in Ref. [2]. Nb and Ti metals with a purity of 99.99% were used and the alloy ingots were prepared in an argon-levitation melting furnace with a cold crucible. The Ti loss problem can be effectively avoided with levitation furnace since the molten metal does not contact with the crucible during melting process [15]. The investigated alloys contained 0.75, 25, 45 and 74 at % Ti. The prepared Nb–Ti alloy ingots were segmented and remelted with the addition of TiO_2 powder in order to obtain the desired Nb–Ti–O alloys. The alloys were analyzed by means of energy dispersive X-ray spectroscopy. Table 1 shows the chemical compositions of four of the investigated alloys.

Beam-shaped samples of dimensions $1 \times 10 \times 60$ mm^3 were used for internal friction (Q^{-1}) measurements on a dynamic mechanical analyzer (DMA-2980, TA Instrument, Inc.). A forced vibration in the dual-cantilever mode was applied to the samples. The temperature range of the measurements extended from 10 to 450°C and the heating rate and frequency were 2 °C/min and 1 Hz, respectively.

The peak of Snoek relaxation can be described by the following expression [1]:

$$Q^{-1}(T) = \sum Q_m^{-1} \sec h \left[\frac{H}{R}\left(\frac{1}{T} - \frac{1}{T_m}\right)\right] \quad (1)$$

where H is the activation enthalpy, Q_m^{-1} and T_m are the peak height and temperature, respectively. The decomposition of the complex curves into constitutive peaks was realized using Eq. 1 by specifying a set of parameters H, Q_m^{-1} and T_m. The most reliable of these parameters was fixed, while the others were varied until the best fit to the experimental curve was achieved.

The linear correlation between H and T_m for a Snoek-like peak, i.e. the so-called Wert-Marx equation [16], was used as the coupled-equation of Eq. 1. The aim was to reduce the speculatitve nature of the fitting procedure.

$$H(T_m) = RT_m \ln\left(kT_m/hf_m\right) + T_m \Delta S \quad (2)$$

where k and h are the Boltzmann and Plank constants. For the entropy of activation ΔS a value of 1.1×10^{-4} eV/K was used as it gave the best matching with those deduced from the Arrhenius plot of the Snoek relaxation [17].

The elementary isolated Snoek peak proves to be broader than the theoretical one. The spectrum was described by a distribution function $r_2(\beta)$ [1] according to the following expression:

$$Q^{-1}(T) = \sum Q_m^{-1} \sec h \left[\frac{H}{r_2(\beta)R}\left(\frac{1}{T} - \frac{1}{T_m}\right)\right] \quad (3)$$

in which β is the peak broadening parameter and for a single Debye peak $\beta = 0$. It can be shown that the effect on the peak width of a change of β is similar to that of a change of H, in that an increase of β is equivalent to a decrease of H by a factor n, which is the ratio of the half-width of the experimental peak (with a certain β) to that of the ideal peak ($\beta = 0$). Thus, Eq. 3 can be rewritten as:

$$Q^{-1}(T) = \sum Q_m^{-1} \sec h \left[\frac{H}{nR}\left(\frac{1}{T} - \frac{1}{T_m}\right)\right] \quad (4)$$

here we define n as the peak shape parameter. Kushnareva suggested an experiential relation between β and n for Nb-based alloys [18, 19]. Adopting this method, we took into account the spread of individual fitting peaks by using values for n between1.01 and 1.8.

Table 1 The chemical compositions of the as-cast Nb–Ti–O alloys (at %)

Alloy	Nb	Ti	Fe	Al	O	C	N
Nb–0.75Ti–1.5O	97.37	0.89	0.015	0.007	1.705	0.004	0.0062
Nb–25Ti–1.5O	73.71	24.77	0.013	0.009	1.488	0.004	0.0061
Nb–45Ti–1.5O	53.58	44.85	0.022	0.012	1.521	0.004	0.0072
Nb–74Ti–1.5O	25.20	73.73	0.033	0.006	1.705	0.004	0.0065

Results

The Snoek relaxation peak due to O atoms in unalloyed Nb [20, 21] was found at about 431 K (at frequency 1 Hz) and its activation energy is 107 kJ/mol (different works gave this value as ranging from 107 to 117 kJ/mol). This peak, which will be denoted P_0, can be identified firstly in the peak resolution process. With an increase in Ti concentration (C_{Ti}), the peak broadens on the high temperature side. By the fitting procedure a series of additional peaks, denoted as P_1, P_2, ... in sequence, can be identified.

The temperature-dependent curves of internal friction and the fitting results for alloys with 0.75 at % Ti are shown in Fig. 1. For the Nb–0.75 Ti alloy, besides peak P_0, two peaks (P_1 and P_2) could be resolved at about 465 K and 574 K, and the corresponding activation energies H_1 and H_2 are 116 kJ/mol and 144 kJ/mol, respectively. It can be seen that the fitting curve is in good coincidence with the experimental one. The shape parameter n and the broadening parameter β of peak P_0 are 1.03 and 0.3[18], respectively. It indicates that the shape of P_0 is close to ideal.

The results for the Nb–25Ti alloy are shown in Fig 2a. Besides P_0, P_1 and P_2, an additional peak, P_3, appears at about 518 K whose activation enthalpy H_3 is equal to 129 kJ/mol. Different from the Nb–0.75Ti alloy, peak P_2 was the biggest one among the fitting elementary peaks in this alloy. The situation for alloy Nb–45Ti (Fig 2b) is similar to that for alloy Nb–25Ti. All four peaks P_0, P_1, P_2 and P_3 are present in the fitting result. However, the relative height of the elementary peaks has remarkably changed, peak P_3 being the highest one in this case.

In comparison to the above alloys, the experimental peak width of Nb–74Ti alloy was smaller and the peak shape became more symmetrical. As shown in Fig 3, peak

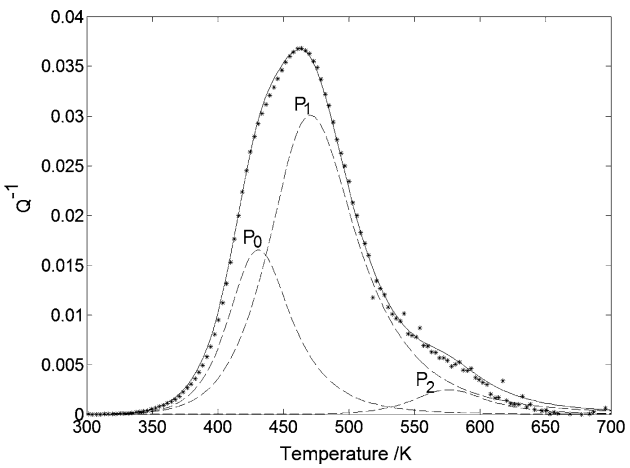

Fig 1 Temperature dependence of internal friction (at 1 Hz) and the fitting results in Nb–0.75Ti–1.5O (points–experimental; dashed line—fitted elementary peaks; solid line—the sum of the elementary peak)

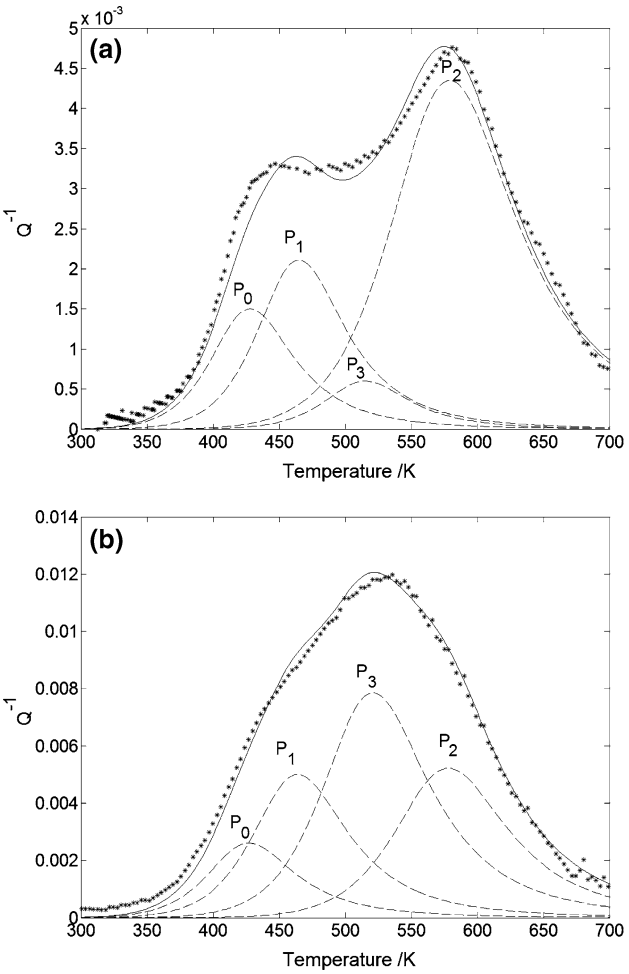

Fig 2 Temperature dependence of internal friction (at 1 Hz) and the fitting results in: (**a**) Nb–25Ti–1.5O; (**b**) Nb–45Ti–1.5O (points–experimental; dashed line—fitted elementary peaks; solid line—the sum of the elementary peak)

P_0 disappeared and P_2 became very trifling. A huge peak P_4 formed at about 486 K and its activation enthalpy H_4 was about 121 kJ/mol.

The fitting parameters (T_m, H and n) in Nb–Ti–O alloys at 1 Hz are summarized in Table 2. The broadening parameter β of each peak determined by the Kushnareva method [18] are also listed. One can see that, with increasing the numbering of the peak index j, the value of broadening parameter β increases. This indicates a larger broadening effect on the higher numbering peaks, which appear in the high Ti content alloys.

Discussion

The nature of the elementary peaks (P_j)

It can be seen that, in Nb–Ti alloys (with up to 74 at% Ti) O gives rise to several elementary Snoek peaks at different

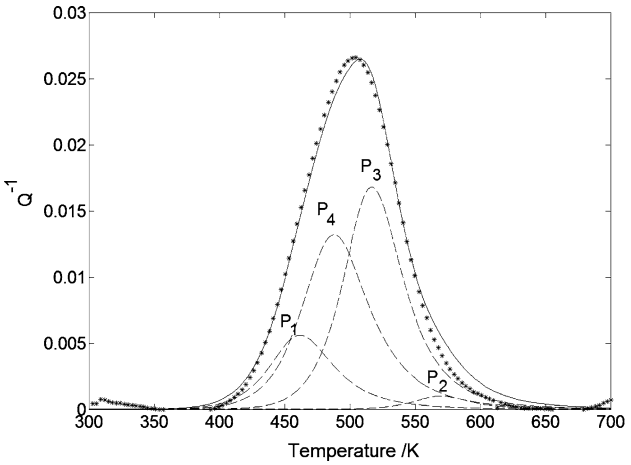

Fig 3 Temperature dependence of internal friction (at 1 Hz) and the fitting results in Nb–74Ti–1.5O. (points–experimental; dashed line—fitted elementary peaks; solid line—the sum of the elementary peak)

Table 2 Parameters of elementary peaks in Nb–Ti–O alloys (1 Hz)

Peaks $P_j (j = 0–4)$	P_0	P_1	P_2	P_3	P_4
$T_{m,j}$ (K)	430	465	574	518	486
H_j (KJ/mol)	107	116	144	129	121
n/β	1.03/0.3	1.29/1.1	1.44/1.4	1.66/1.75	1.65/1.75

temperatures. The number of the peaks varies with the Ti content. Thus, the O relaxation peak in Nb–Ti alloys is obviously perturbed by the presence of Ti.

In Nb–Ti–O alloys, an octahedral interstitial O atom is surrounded by two nearest and four next-nearest neighbor atoms, which may be host (Nb) or substitutional solute (Ti) [22]. The situation is illustrated in Fig. 4. Therefore, as a result of the introduction of Ti into Nb, the octahedral interstitial sites can be classified in seven types, differing in the number (j) of Ti atoms (j = 0–6). The number of distinguishable sites becomes eighteen if the symmetry features

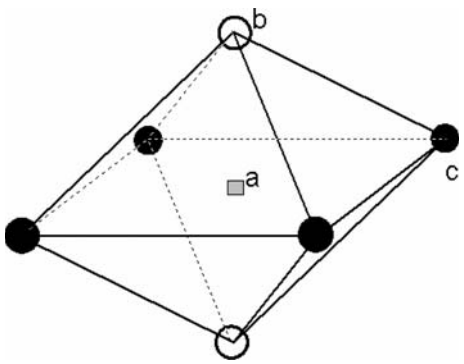

Fig 4 Schematic of a octahedral cell in BCC lattice. (■—interstitial site; ○—nearest neighbor sites; ●—next-nearest neighbor site)

associated with the distribution of substitutional solutes among the six neighbor lattices sites are also take into account [23]. Different types of interstitial O atoms have different relaxation characteristics. These facts have been confirmed by results of the analysis of peaks in Nb–Zr–N [24], Nb–V–O [25, 26] and Fe–Cr(Al)–C(N) [17, 27] alloys.

Pick's method [28] for calculating the fraction of the various types of octahedral sites in a random solid solution has been applied to the present system. For convenience, we shall label these different types of sites (cells) as $Nb_{6-j}Ti_j$. Since each matrix atom (Nb or Ti) has three octahedral interstitial sites, the number of the different cells (n_j) can be calculated based on the statistical occupation probabilities of the matrix atoms:

$$n_0 = 3N(1-C)^6 \tag{5.1}$$

$$n_1 = 3N6C(1-C)^5 \tag{5.2}$$

$$n_2 = 3N15C^2(1-C)^4 \tag{5.3}$$

$$n_3 = 3N20C^3(1-C)^3 \tag{5.4}$$

$$n_4 = 3N15C^4(1-C)^2 \tag{5.5}$$

$$n_5 = 3N6C^5(1-C) \tag{5.6}$$

$$n_6 = 3NC^6 \tag{5.7}$$

where N is the total number of matrix atoms and C is the concentration of substitutional atoms. The total number of different octahedral cells (n_t) should be:

$$n_t = \sum_{j=0}^{6} n_j \tag{6}$$

The fraction of cells of type j can be calculated as $h_j = n_j/n_t$. The results for the Nb-0.75, 25, 45 and 74 at % Ti are listed in Table 3.

Based on data in Table 3 we can discuss the experimental and fitting results. It can be seen that in the Nb–0.75 Ti alloys: 6.41% of the cells contain on Ti atom (Nb_5Ti) and about 0.18 % contain two Ti (Nb_4Ti_2), and the residual are cells of type Nb_6. Following Szkopiak [10], we explain peak P_1 as being due to O atoms located in cells of type j = 1. Lauf estimated [29] that the binding energy of substitutional Ti–O in diluted Nb alloy could be as high as 0.7 eV; this means that Ti atoms would act as strong traps

Table 3 The fraction of octahedral cells with various numbers of Ti neighbours

C_{Ti} (at%)	h_j						
	0	1	2	3	4	5	6
0.75	0.9341	0.0641	0.0018	–	–	–	–
25	0.1780	0.3560	0.2966	0.1318	–	–	–
45	0.0281	0.1373	0.2791	0.3027	0.1846	–	–
74	–	0.0053	0.0375	0.1424	0.3041	0.3642	0.1642

for O and would give rise to a large Ti–O interaction peak. The small peak P_2 at 574 K in Fig. 1 could be attributed to the small fraction of O atoms located inside the type $j = 2$ cells.

For the Nb–25Ti alloy, cells containing three Ti atoms (Nb_3Ti_3) are also present and their fraction is 13.18%. As a result, peak P_3 appears at 518 K (Fig 2a). The situation of the Nb–45Ti alloy is similar. In this case, the cells of type $j = 3$ became preponderant (fraction = 30.27%), thus, most of the O atoms should be trapped in the $j = 3$ type of cells. This is the reason why peak P_3 became the highest in Fig 2b.

Let us now turn to the Nb–74Ti alloy. There are no cells of type $j = 0$ in this alloy. As a result, peak P_0 disappeared in Fig. 3. About 83.25% of the cells in this alloy are of type $j \geq 4$, thus we attribute the huge peak P_4 occurring at 486 K to reorientation of O atoms located within cells with four or more substitutional Ti atoms. Based on the present fitting method, the experimental curve of Nb–74Ti alloy can not be resolved into a higher elementary peaks with index higher than 4. The reason may be that O atoms have similar distribution probabilities and similar relaxation parameters in cells that contain more than 4 Ti atoms.

One may notice that the broadening parameter β of fitting peaks increase with the numbering of the peak j. This is a quite reasonable result. For the peak P_0, all six neighbor sites of the interstitial O atom are occupied by Nb atoms, therefore, only one configuration exists for this cell. However, with increasing the number j, multiform configurations of matrix atoms can occur. For example, cells of type Nb_5Ti may have two configurations ($\beta_1 = 1.1$) and Nb_4Ti_2 may have four configurations ($\beta_2 = 1.4$) since Ti atoms can occupy different symmetry sites among the six nearest and next nearest lattice sites. These factors will lead to a scatter in the relaxation time τ_j and result in a broadening effect on the corresponding peak. The situation is shown in Figs. 5 and 6.

Kushnareva thought that [21], compared to the difference between τ_j and $\tau_{j\pm1}$, the difference in τ_j for the cells with the same j but different configuration was rather small. In addition, a more energy-favorable configuration, among the possible configurations of a cell, would exist in a higher probability. Therefore, for a certain type of octahedral cell, only one broadened elementary peak can be resolved, rather than a series of separate peaks.

It should be pointed out that, here the transition of interstitial atoms was assumed to be a confined-reorientation in one octahedral cell. The actual situation is more complicated [23] since a Snoek transition of interstitial atoms occur between two adjacent octahedral cells.

The influence of Ti–O interactions

As it has been seen, substitutional Ti solutes will markedly influence the relaxation behavior in Nb–Ti–O alloys. Such an effect is most likely due to the interaction between substitutional Ti and interstitial O atoms. This interaction will determine the site energy of O interstitial atoms in different cells. Here an embedded cell model [30] is used to calculate the octahedral site energy of O atoms in ternary Nb–Ti–O alloys, and the calculation results are used to estimate the influence of the Ti–O interaction on the relaxation peaks.

In principle, an octahedral cell $Nb_{6-j}Ti_j$ can be treated as an alloy with local concentration $y' = j/6$ embedded into the alloy matrix $Nb_{1-y}Ti_y$ with concentration y (as shown in Fig. 7). The site energy is assumed to depend predominantly on the difference between the cell local component and the matrix. It is composed of two main parts: (i) the elastic interaction of the local strain field (ε) of a cluster in the matrix alloy, and (ii) the chemical affinity (Λ) between interstitial atoms and the nearest neighbor metal atoms, i.e.:

$$E_j = E_j(\Lambda) + E_j(\varepsilon) \quad (j = 0, 1, \ldots, 6) \tag{7}$$

According to the embedded cell method, the elastic interaction part of the site energy ($e_u^O(\varepsilon)$) of an octahedral interstitial site in a ternary BCC alloy can be expressed as:

$$E_j(\varepsilon) = \Omega(1-D)\left[(1-y)\,V_{Nb} + yV_{Ti} - \frac{(6-j)V_{Nb} + jV_{Ti}}{6}\right] \tag{8}$$

where V_{Nb} and V_{Ti} are the cell volume of Nb_6 and Ti_6 in the pure metals. Ω is the bulk modulus of the alloy which can be estimated by $\Omega = (1-y)\ \Omega_{Nb} + y\Omega_{Ti}$. The parameter $D \in [0, 1]$ and represents the force constant between nearest neighbor atoms.

Analogous to Eq. 8, the chemical affinity (Λ) can be estimated by the following expression:

$$E_j(\Lambda) = (y - j/6)\Lambda \tag{9}$$

where $\Lambda = \Delta H^f_{NbO} - \Delta H^f_{TiO_2}$. ΔH^f_{NbO} and $\Delta H^f_{TiO_2}$ are the heat of formation (ΔH^f) of NbO and TiO_2 respectively.

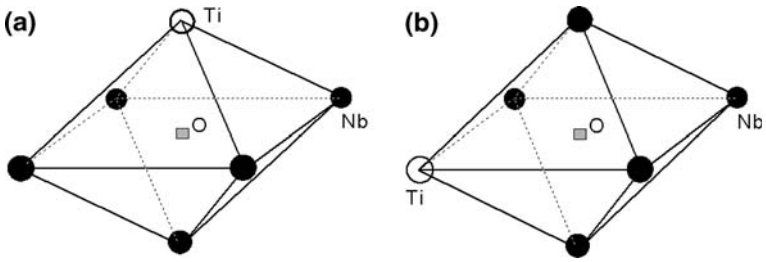

Fig 5 Schematic configurations of octahedral cell Nb_5Ti: (**a**) Ti atom occupy the nearest site; (**b**) Ti atom occupy the nest-nearest site (■—interstitial O atoms; ○—Ti; ●—Nb)

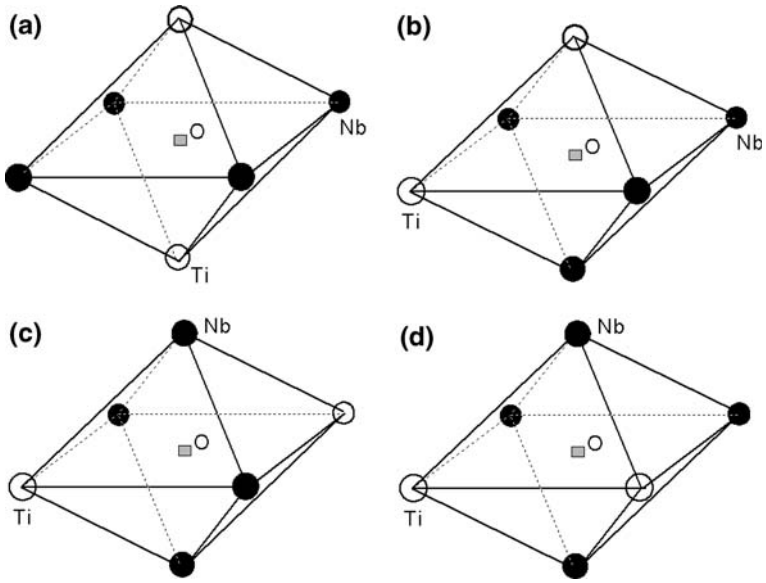

Fig 6 Four possible configurations of octahedral cell Nb_4Ti_2 (■—interstitial O atoms; ○—Ti; ●—Nb)

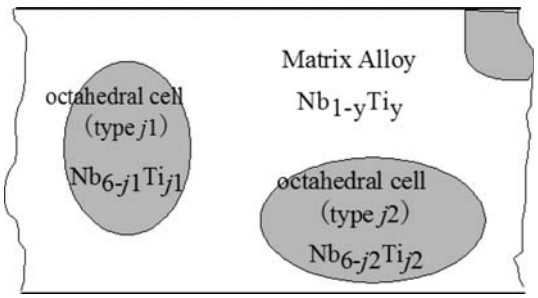

Fig. 7 Schematic representation of the embedded-cell model. An octahedral cell $Nb_{6-j}Ti_j$ is treated as an alloy with local concentration $y' = u/6$, and embedded into the matrix alloy $Nb_{1-y}Ti_y$ with the concentration y

Here we apply this procedure to the Nb–Ti–O alloy system. The calculated values of E_j are plotted versus alloy composition in Fig. 8.

It is worth noting that the energy of a given site depends on the average composition of the alloy matrix, and Ti_6 site is the most energetically favorable for O occupancy compared to other sites. Since Nb and Ti have similar atomic radius, the elastic interaction is negligible. The main contribution to the site energies is due to chemical affinity. In this system, Ti substitutional solute has a higher affinity for O than the host element Nb, therefore, O atom tends to distribute over the octahedral cells which contain more Ti solutes.

The thermodynamic equilibrium concentrations (c_j) of the O atoms in different cells could be described using the Maxwell–Boltzmann statistical equation:

$$c_j = \frac{h_j \exp\left(-E_j/kT\right)}{\sum_{i=0}^{6} h_i \exp(-E_i/kT)} \tag{10}$$

Substituting Eq. 7, 8 and 9 into Eq. 10, leads to a set of nonlinear equations in the unknown quantities c_j. With the boundary condition $C = \sum_{j=0}^{6} c_j$, the normalized site concentrations c_j/C, calculated as a function of Ti content (y) in $Nb_{(1-y)}Ti_y$ for different temperatures, are shown in Fig. 9.

It can be seen that interstitial O atoms preferentially occupy the octahedral interstitial site, which have nearest-neighbors Ti atoms due to the Ti–O interaction. For example, in the Nb–0.75Ti–1.5O (at%) alloy, the fraction of octahedral cell Nb_6, is 93.41%, however, only 33.35 % of O atoms distributed over these cells. Most of O atoms occupy cells of type Nb_5Ti and Nb_4Ti_2. Therefore, substitutional Ti solutes will markedly influence

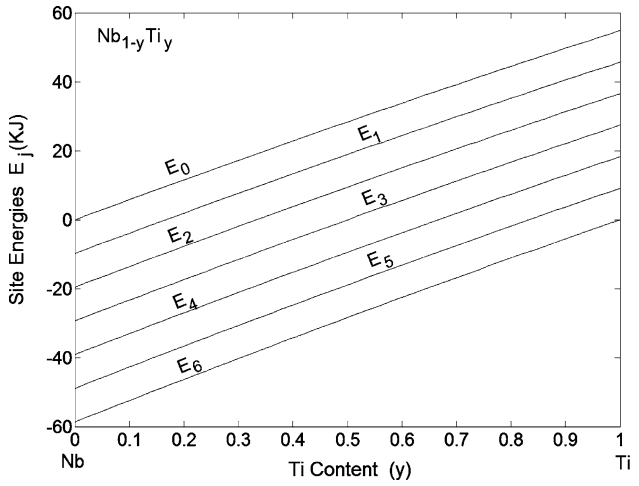

Fig. 8 Octahedral site energy E_j of oxygen atoms in Nb-Ti alloys as a function of alloy composition. Curves are calculated with the embedded-cell model. The parameters [29, 30] used in the calculations are: $V_{Nb} = 10.8$ cm^3/mol, $V_{Ti} = 10.6$ cm^3/mol, $\Omega_{Nb} = 171$ KJ/cm^3, $\Omega_{Ti} = 95$ KJ/cm^3, $\Lambda = -50.1$ KJ/cm3, $D = 0.75$

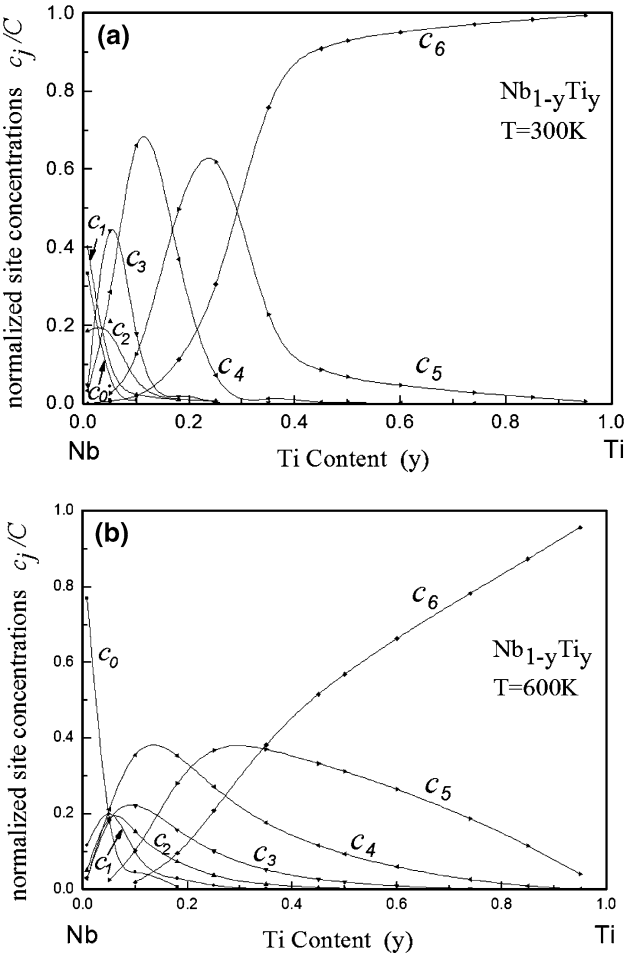

Fig. 9 The octahedral site concentration c_j of oxygen atoms in Nb–Ti alloys at different temperatures. (**a**) at 300 K; (**b**) at 600 K

the Snoek relaxation behavior in Nb–Ti–O ternary system, even if the concentration of Ti is rather low. At higher temperature (Fig. 9b), occupancies of higher energy sites become appreciable and may contribute to the anelastic relaxation. As a result, the Snoek peak will be broadened, asymmetric, or even new peaks may appear, especially in the alloys containing higher concentrations of Ti substitutional solutes.

Conclusions

(1) The complicated internal friction peak of Nb–Ti–O alloys can be resolved into several elementary quasi-Debye peaks, and each peak corresponds to reorientation of O atoms sitting in certain octahedral cells, containing j (j = 0... 6) substitutional Ti atoms. The number and the kind of peaks depend upon the Ti concentration. The broadening effect increases with increasing the numbering of the elementary peak.

(2) The interstitial oxygen atoms preferentially occupy the octahedral interstitial site which has Ti substitutional atoms as nearest-neighbors. This effect happens due to the Ti-O interaction. Therefore, substitutional Ti solutes markedly influence the Snoek relaxation behavior in the Nb–Ti–O ternary alloys.

References

1. Nowick AS, Berry BS (1972) Anelastic relaxation in crystalline solids. Academic Press, New York, Chapter 9 and 11.
2. Yin FX, Iwasaki S, Ping DH, Nagai K (2006) Adv Mater 18:1541
3. Dijkstra LJ, Sladek RJ (1953) Trans Metall AIME 197:69
4. Berry BS (1962) Acta Metall 10:271
5. Nowick AS, Heller WR (1963) Adv Phys 12:251
6. Koiwa M (1971) Philos Mag 24:81
7. Blanter MS, Fradkov MY (1992) Acta Metall Mater 40:2201
8. Ahmad MS, Szkopiak ZC (1970) J Phys Chem Solids 31:1799
9. Weller M, Zhang JX, Li GY, Ke TS, Diehl J (1981) Acta Metall 29:1055
10. Szkopiak ZC, Smith JT (1975) J Phys D 8:1273
11. Cantelli R, Szkopiak ZC (1976) Appl Phys 9:153
12. Florencio O, Botta WJ, Grandini CR, Tejima H, Jordao JAR (1994) J Alloy Compd 211/212:37
13. Almeida LH, Niemeyer TC, Pires KCC, Grandini CR, Pintao CAF, Florencio O (2004) Mat Sci Eng A 370:96
14. Niemeyer TC, Grandini CR, Florencio O (2005) Mat Sci Eng A 396:285
15. Morita A, Fukui H, Tadano H, Hayashi S, Hasegawa J, Niinomi M (2000) Mat Sci Eng A 280:208
16. Wert C, Marx J (1953) Acta Metall 1:113
17. Golovin IS, Neuhauser H, Riviere A (2004) Intermetall 12:125
18. Kushnareva NP, Pecherskii VS (1984) Ind Lab 50(4):371
19. Gridnev VN, Kushnareva NP, Pecherskii VS, Yakovenko PG (1983) Phys Met Metall 56:93
20. Florencio O, Grandini CR, Botta WJ, Guedes PR, Silva PS (2004) Mat Sci Eng A 370:131

21. Kushnareva NP, Snejko SE, Yarosh IP (1995) Acta Metall Mater 43:4393
22. Beshers DN (1965) J Appl Phys 36:290
23. Biscarini A, Coluzzi B, Mazzolai FM (1999) Def Diff Forum 165–166:1
24. Mosher D, Dollins C, Wert C (1970) Acta Metall 18:797
25. Indrawirawan H, Buck O, Carlson ON (1987) Phys Stat Sol (a) 104:443
26. Kushnareva NP, Snejko SE (1994) J Alloy Compd 211/212:75
27. Gondi P, Montanari R (1992) Phys Stat Sol (a) 131:465
28. Pick MA, Shapiro SM, Stoneham AM (1986) J Phys F 16:961
29. Lauf RJ, Alstetter CJ (1979) Acta Metall 27:1157
30. Brouwer RC, Griessen R (1989) Phys Rev B 40:1481